Depolarization of backscattered linearly polarized light

Luis Fernando Rojas-Ochoa

Department of Physics, University of Fribourg, CH-1700 Fribourg, Switzerland

David Lacoste

Physico-Chimie Théorique, Ecole Supérieure de Physique et de Chimie Industrielles (ESPCI), 10 Rue Vauquelin, 75231 Paris Cedex 05, France

Ralf Lenke

Fakultät für Physik, Universität Konstanz, D-78547 Konstanz, Germany, and Carl Zeiss Laser Optics GmbH, D-73446 Oberkochen, Germany

Peter Schurtenberger and Frank Scheffold

Department of Physics, University of Fribourg, CH-1700 Fribourg, Switzerland

Received January 29, 2004; revised manuscript received March 24, 2004; accepted April 15, 2004

We formulate a quantitative description of backscattered linearly polarized light with an extended photon diffusion formalism taking explicitly into account the scattering anisotropy parameter g of the medium. From diffusing wave spectroscopy measurements, the characteristic depolarization length for linearly polarized light, l_p, is deduced. We investigate the dependence of this length on the scattering anisotropy parameter g spanning an extended range from -1 (backscattering) to 1 (forward scattering). Good agreement is found with Monte Carlo simulations of multiply scattered light. © 2004 Optical Society of America

OCIS codes: 290.4210, 030.5620, 260.5430.

1. INTRODUCTION

Polarized light scattered many times in a random medium leaves the sample partially depolarized. Unfortunately, despite its importance in areas such as biomedical optical imaging, coherent backscattering, or dynamic spectroscopy,[1–4] the depolarization of light in a random medium is still not completely understood because of the complexity of vector wave multiple scattering (as compared with the much simpler problem of scalar wave propagation). Previous attempts have mainly focused on isotropic (Rayleigh) scattering[5] or on the depolarization of circularly polarized light.[4,6] Only a few studies have discussed specifically the mechanism of depolarization of linearly polarized light in the case where the anisotropy parameter $g = \langle \cos\theta \rangle$ is different from 0, and furthermore a detailed comparison with experiment has been lacking.[7–13] An accurate description for arbitrary scattering anisotropy is, however, crucial for analyzing the information contained in backscattered light if progress is to be made in applications such as remote sensing, photon correlation spectroscopy, or optical imaging of biological tissues.[1,14,15]

In this paper we formulate a quantitative description of backscattered linearly polarized light by using an extended photon diffusion formalism taking explicitly into account the scattering anisotropy parameter g. The details of our model are adjusted by comparison with Monte Carlo simulations of multiply scattered light. We show how the characteristic length of depolarization of incident linearly polarized light, l_p, can be deduced from measurements of intensity fluctuations of light scattered from liquid turbid media by means of diffusing wave spectroscopy (DWS). We can distinguish the following limiting situations for the transport of light and its polarization: isotropic scattering ($g \simeq 0$), forward-peaked scattering ($g \simeq 1$), and backward-peaked scattering ($g \simeq -1$). The situation of forward-peaked scattering ($g \simeq 1$) is typical of Mie scattering[16,17] with large particles and of biological tissues, whereas the situation of $g < 0$ has been made possible experimentally only recently by tuning the interaction of the light with the use of mesostructured colloidal liquids.[18] Here we show that with our additional correction the simple photon diffusion picture successfully describes the distribution of path lengths and the DWS autocorrelation function in the backscattering geometry.

2. PATH-LENGTH DISTRIBUTION FOR BACKSCATTERING

On length scales much larger than the transport mean free path l^*, the transport of light in a turbid medium can be described by the diffusion approximation. This approximation is connected to the idea of treating the transport of photons as a random walk, characterized by a dis-

tribution of path lengths.[5,19–21] An exact solution of the diffusion equation applied to light transport can be obtained with the method of images. This method takes into account the boundary conditions through two lengths, which are both of the order of a transport mean free path: the extrapolation length z_e, where the flux of photons vanishes outside the sample, and z_p, which is the location of the photon source (for a more detailed interpretation of z_e, z_p based on a random-walk model, see Ref. 4). The method leads to

$$P(s) = \frac{\sqrt{3}}{4\sqrt{\pi l^* s^{3/2}}}\left\{ z_p \exp\left(-\frac{3}{4}\frac{{z_p}^2}{l^* s}\right) + (z_p + 2z_e)\exp\left[-\frac{3}{4}\frac{(z_p + 2z_e)^2}{l^* s}\right]\right\}, \quad (1)$$

which obeys the normalization condition $\int_0^\infty P(s)\mathrm{d}s = 1$. Note that the path length is simply related to the number of scattering events n by $s/l = n - 1$, so that the path length is 0 for single scattering. Here l is the scattering mean free path. Both quantities, l and l^*, are related by $l^*/l = 1/(1 - g)$. The scattering anisotropy parameter g is defined as the average of the cosine of the scattering angle: $g = \langle \cos \Theta \rangle$.

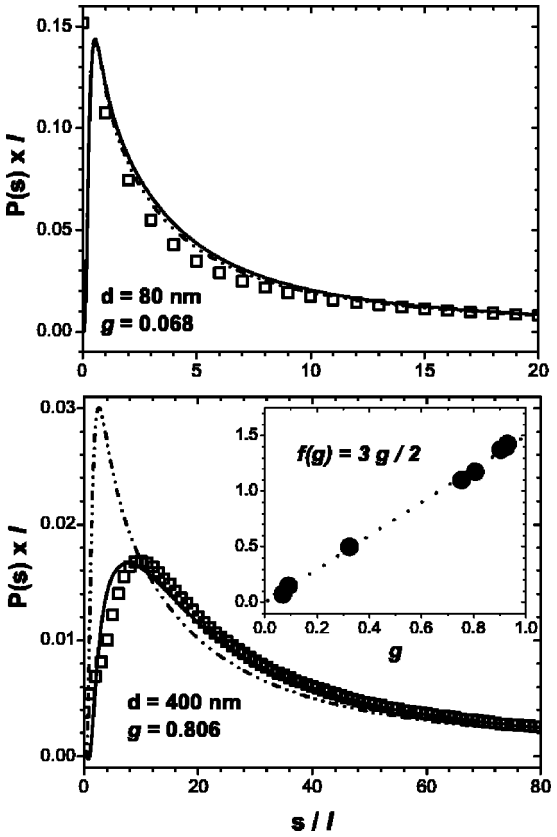

Fig. 1. Normalized path-length distribution $P(s) \times l$ for backscattered light from a semi-infinite medium. The symbols refer to Monte Carlo simulations, and the curves are calculations based on relation (2) with $f(g) = 3g/2$ (solid) and $f(g) \equiv 0$ (dashed). Inset: $f(g)$ obtained from Eq. (1) adjusted to fit the simulation results. The wavelength is $\lambda_0 = 532$ nm, and the refractive indices are $n_p = 1.59$ of the particle and $n_s = 1.332$ of the solvent. Nonreflecting boundary conditions were used.

To check the validity of Eq. (1), we have performed Monte Carlo simulations of linearly polarized light reflected from a semi-infinite turbid medium (details about the simulation method can be found in Refs. 4, 22, and 23. These simulations use the Mie scattering cross section in the range $0 \leqslant g \leqslant 1$ and are able to evaluate numerically an exact path-length distribution as a function of the number of scattering events n and of the polarization. The simulations were done for uncorrelated spherical scatterers [structure function $S(q) \equiv 1$] and for a nonreflecting interface. Values of $\lambda_0 = 532$ nm for the incident wavelength, $n_p = 1.59$ for the refractive index of the particle and $n_s = 1.332$ for the solvent refractive index, were used. In Fig. 1 we compare the results of the simulations with the prediction of the method of images according to Eq. (1). We see clearly in this figure that the method of images provides an excellent description of the path-length distribution for the case of isotropic scattering ($g \equiv 0$) but that the method fails to give an equally good description for the case of anisotropic scattering corresponding to $g \simeq 0.806$.

The disagreement in the latter case is not surprising, as the diffusion approximation is known to overestimate the contribution from the short paths of the distribution, the error becoming more and more severe as the anisotropy of scattering increases. One way to improve the distribution of path lengths of Eq. (1) is by introducing a cutoff into the distribution as suggested by MacKintosh and John.[8] Here we extend their approach by taking into account explicitly the scattering anisotropy factor g [with $\int_0^\infty P_{\mathrm{corr}}(s)\mathrm{d}s = 1$]:

$$P_{\mathrm{corr}}(s) \propto P(s)[1 - f(g)\exp(-s/l^*)]. \quad (2)$$

According to MacKintosh and John,[8] $f(1)$ is of order unity and for isotropic scattering ($g \to 0$) there is no correction [$f(0) = 0$]. Using the corrected distribution of path lengths to fit the simulation results, we have found that the function f is well approximated by a linear dependence $f(g) = 3g/2$, which we assume to be valid also for $g < 0$. As can be seen in Fig. 1, the use of the correction factor significantly improves the prediction of Eq. (1). We note that, alternatively, for the case of forward-peaked scattering ($g \simeq 1$), other schemes of approximations have been suggested. For example, the recent Ref. 13 reports that the Fokker–Plank equation provides a better description than does the (uncorrected) diffusion approximation for forward-peaked scattering.

3. DEPOLARIZATION LENGTH FOR LINEAR POLARIZATION

Incident polarized light loses its polarization in random multiple scattering.[5,7–9,12] For linearly polarized light, only two configurations ($\parallel$ and $\perp$) need to be considered (for isotropic samples). Physically, in the $\parallel$ geometry more photons are detected for short paths as compared with the unpolarized case. In a seminal paper Akkermanns *et al.*[5] found that the path-length distribution for the two configurations can be written as

$$P_{\parallel,\perp}(s) = d_{\parallel,\perp}(s)P(s), \quad (3)$$

with the depolarization ratio given by

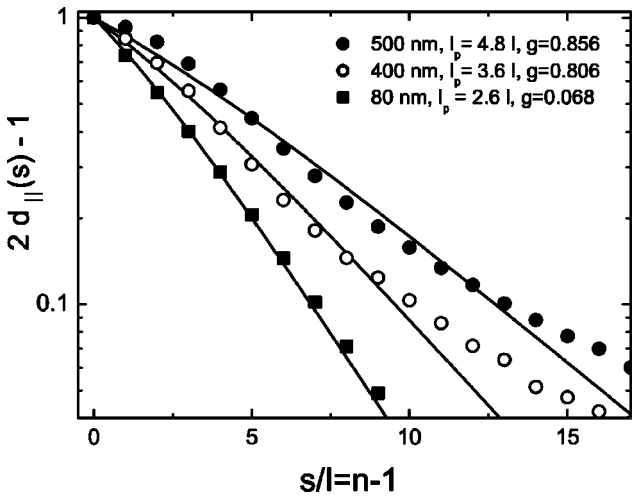

Fig. 2. Depolarization of multiply scattered light: $2d_{\parallel}(s) - 1$ from theory [Eq. (4), curves] and simulation (symbols). Excellent agreement is found for Rayleigh scatterers, while for larger particles the agreement becomes somewhat less good.

$$d_{\parallel}(s) = \frac{1 + 2\exp(-s/l_p)}{2 + \exp(-s/l_p)}, \tag{4}$$

$$d_{\perp}(s) = \frac{1 - \exp(-s/l_p)}{2 + \exp(-s/l_p)}, \tag{5}$$

in terms of the characteristic length of depolarization for linearly polarized light, l_p. For pointlike scatterers ($g = 0$) Akkermans *et al.* obtained $l_p = l/\ln(10/7) \cong 2.804l$[5]. We find good agreement between Eq. (3) and our numerical simulations with l_p as an adjustable parameter (Fig. 2). For large particles (and therefore large g), the agreement is somewhat less good. However, polarization effects in DWS are usually found weak for $g \approx 1$, and therefore we did not attempt to improve the accuracy of Eqs. (4) and (5). (It is worthwhile to note that for diffuse backscattering, interesting polarization effects persist for $g \approx 1$ if the speckle pattern is analyzed in the image plane rather than in the far field.[11,24,25]

In the limit $s/l \gg 1$ Eqs. (4) and (5) reduce to

$$P_{\parallel,\perp}(s) \cong [\tfrac{1}{2} \pm \tfrac{3}{4}\exp(-s/l_p)]P(s). \tag{6}$$

We consider this expression the simplest generalization, since it captures well intermediate path lengths ($s/l > 3$), where polarization effects are important, but at the same time the number of scattering events is already sufficiently large to apply the diffusion approximation.

4. POLARIZATION DEPENDENCE OF DIFFUSING WAVE SPECTROSCOPY AUTOCORRELATION FUNCTION

In transmission geometry the path-length distribution can be measured experimentally with pulsed laser beams.[26] In reflection, however, paths are short, and therefore the time resolution is usually not sufficient for such measurements. An alternative way to probe diffuse light propagation is the analysis of temporal fluctuations of the scattered light by means of photon correlation spectroscopy. This approach, called diffusing wave spectroscopy (DWS), is a sensitive probe to the path-length distribution, in particular in reflection geometry.[2,3] The temporal intensity correlation function $g_2(t)$ that is measured is related to the field autocorrelation function by the Siegert relation $g_1(t) = [1 - g_2(t)]^{1/2}$. The latter is directly related to the path-length distribution:

$$g_1(t) = \int_0^{\infty} P(s)\exp[-2(t/\tau_0)s/l^*]\mathrm{d}s. \tag{7}$$

In our case the characteristic relaxation time for diffusive particle motion (short-time diffusion constant D for Brownian motion), $\tau_0 = (k_0{}^2D)^{-1}$, is a known quantity. The path-length distribution $P(s)$, as given by Eq. (1), has been derived for the case of a semi-infinite nonabsorbing medium. For real systems both absorption and limited container size lead to a loss of photons along a given path. For such cases the path-length distribution becomes $P'(s) = \exp(-s/l_a)P(s)$, where l_a is the characteristic absorption length of the medium. In this framework, absorption can be taken into account by the modification

$$6t/\tau_0 \rightarrow 6t/\tau_0 + 3l^*/l_a \tag{8}$$

in Eq. (7).[1] All our experiments correspond to the case where l_a is much larger than l^*.

The solution for the scalar (polarization-independent) path-length distribution is well-known[1] (neglecting absorption): $g_1(t) = \{\exp[-\gamma_p x(t)] + \exp[-(\gamma_p + 2\gamma_e)x(t)]\}/2$, where $x(t) = (6t/\tau_0)^{1/2}$, $\gamma_p = z_p/l^*$, and $\gamma_e = z_e/l^*$. In the limit $x \ll 1$ it reduces to

$$g_1(t) = \exp(-\gamma x), \tag{9}$$

with $\gamma = -\partial(\ln g_1)/\partial x|_{x=0} = \gamma_p + \gamma_e$. Note that this expression is independent of l^* and that, for the nonreflecting interface that we have considered;

$$\gamma = 1 + z_e/l^* = 5/3. \tag{10}$$

All different paths of length s contribute to $g_1(t)$. Short paths predominantly contribute to the long-time decay, and long paths contribute to the short-time decay. Clearly, polarization effects modify the path-length distribution and therefore strongly influence the decay of $g_1(t)$. Interestingly, the shape of $g_1(t)$ remains more or less unchanged. In most previous studies Eq. (9), though derived for the scalar case, has also been applied with polarized light. Although γ is in principle a well-defined constant, it has been treated in the literature as an adjustable parameter to explain the polarization dependence of the correlation function. Values of $\gamma_{\perp,\parallel}$ in the range 1–3 have been reported, the actual value depending on detected polarization state, particle size, and concentration.[1,7,27]

Rather than adjusting the parameter γ, we take into account the polarization by means of relation (6) and find that

$$g_{1\perp}(t) = \frac{\int_0^\infty P_\perp(s)\exp[-2(t/\tau_0)(s/l^*)\mathrm{d}s]}{\int P_\perp(s)\mathrm{d}s},$$

$$g_{1\parallel}(t) = \frac{\int_0^\infty P_\parallel(s)\exp[-2(t/\tau_0)(s/l^*)\mathrm{d}s]}{\int_0^\infty P_\parallel(s)\mathrm{d}s}. \quad (11)$$

When we introduce the function $2h(x) = \exp(-\gamma_p x) + \exp[-(\gamma_p + 2\gamma_e)x]$, the correlation functions take the form (neglecting absorption)

$$g_{1,\perp}(t) = \frac{h[x_1(t)] - \frac{3}{2}h[y_1(t)] - \frac{3g}{2}h[x_2(t)] + \frac{9g}{4}h[y_2(t)]}{h[x_1(0)] - \frac{3}{2}h[y_1(0)] - \frac{3g}{2}h[x_2(0)] + \frac{9g}{4}h[y_2(0)]}, \quad (12)$$

$$g_{1,\parallel}(t) = \frac{h[x_1(t)] + \frac{3}{2}h[y_1(t)] - \frac{3g}{2}h[x_2(t)] - \frac{9g}{4}h[y_2(t)]}{h[x_1(0)] + \frac{3}{2}h[y_1(0)] - \frac{3g}{2}h[x_2(0)] - \frac{9g}{4}h[y_2(0)]}, \quad (13)$$

where $x_1(t) = (6t/\tau_0)^{1/2}$, $x_2(t) = (6t/\tau_0 + 3)^{1/2}$, $y_1(t) = (6t/\tau_0 + 3l^*/l_p)^{1/2}$, and $y_2(t) = (6t/\tau_0 + 3 + 3l^*/l_p)^{1/2}$. This set of equations provides a direct relation between measurements detecting $\perp$- or $\parallel$-polarized light, thereby eliminating the need to introduce two adjustable parameters $\gamma_{\perp,\parallel}$. We carried out a series of dynamic multiple-scattering experiments to follow the polarization memory of the reflected light intensity. Experiments were realized as described in Ref. 27 but with $\lambda_0 = 532\,\mathrm{nm}$. The sample cells were suspended in a water bath to suppress reflections and to maintain a constant temperature of $T = 22\,^\circ\mathrm{C}$. All samples used were made from monodisperse polystyrene particles ($n = 1.595$) suspended in water ($n_s = 1.332$), except for one case (diameter = 114 nm), where we used a mixture of water and ethanol[18] ($n_s = 1.365$). A detailed description of all samples is given in Table 1.

In Fig. 3 we show a comparison between experiments and our theoretical expressions. For clarity the data are normalized and plotted as a function of $x = (6t/t_0 + 3l^*/l_a)^{1/2} - (3l^*/l_a)^{1/2}$, thus removing contributions from absorption at $x < 0.1$ [relation (8)]. [The absorption length l_a has been chosen such that $\ln g_1(x)$ scales linearly at small x values.] We find that the theory describes our data very well, with the polarization length l_p being the only adjustable parameter. In particular, the availability of suspensions with negative g values allows a rigorous test of the model over the whole interval $-1 \leqslant g \leqslant 1$. Note that we use the theoretically predicted values γ_p, γ_e and do not adjust them to fit the data (as done in all previous work). Depolarization lengths obtained from fits [Eqs. (12) and (13)] to the DWS data and from numerical simulations (Fig. 2) are presented in Fig. 4. We note again that both DWS experiments ($g_{1\perp}$, $g_{1\parallel}$) are well characterized by a single l_p, even for the most extreme case of $g \to -1$.

In the limit $g \simeq 0$ we find good agreement with the predicted theoretical value of Akkermans *et al.*, $l_p/l \cong 2.804$.[5] As the anisotropy parameter g is increased, l_p/l slowly increases as well. In the case of forward-peaked scattering ($g \simeq 1$), we find that $l_p \simeq l^*$ (see also Refs. 9 and 11). This means that as g approaches 1, an increasing number of scattering events is necessary to depolarize backscattered light. Since l_p/l^* remains constant for $g \to 1$, the ratio l_p/l has to increase sharply, as shown in Fig. 4(b). In the case of backward-peaked scattering ($g \simeq -1$), however, the number of scattering events needed for depolarization remains virtually unchanged. The characteristic length scale of depolarization is still the scattering mean free path l (and not l^*!), as in the case of pointlike scatterers. Therefore it is not

Table 1. Diameter as Obtained from Dynamic Light Scattering, Volume Fraction Φ, and Scattering Anisotropy Parameter *g*

Polystyrene Spheres Used in the Experiments		
Diameter (nm)	Φ (%)	g^a
80 ± 5	3.9	0.04
92 ± 15	4.1	0.05
168 ± 5	2.0 → 30.0	0.29 → −0.13
350 ± 12	1.9	0.74
400 ± 8	1.9	0.80
720 ± 14	1.9	0.90
1000 ± 51	2.0	0.92
1500 ± 53	2.0	0.92
114 ± 5	2.5 → 7.4	−0.25 → −0.78

[a] Obtained either from Mie calculations (for hard-sphere interactions as described in Refs. 18 and 27) or from direct measurements (for the diameter = 114 nm charged spheres as described in Ref. 18).

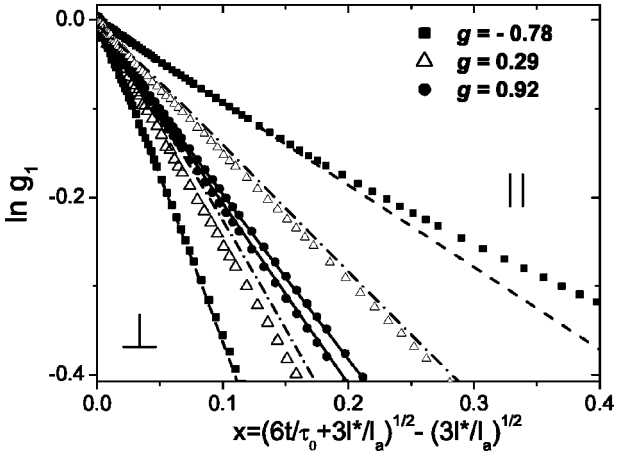

Fig. 3. DWS autocorrelation function for different g values detecting polarized and depolarized light. The lines are calculations based on Eq. (12) with l_p adjusted to fit the data best [($g = -0.78$: $l^*/l_a = 0.004$, $l_p/l^* = 4.83$), ($g = 0.32$: $l^*/l_a = 0.0064$, $l_p/l^* = 2.21$), ($g = 0.924$: $l^*/l_a = 0.016$, $l_p/l^* = 0.713$)].

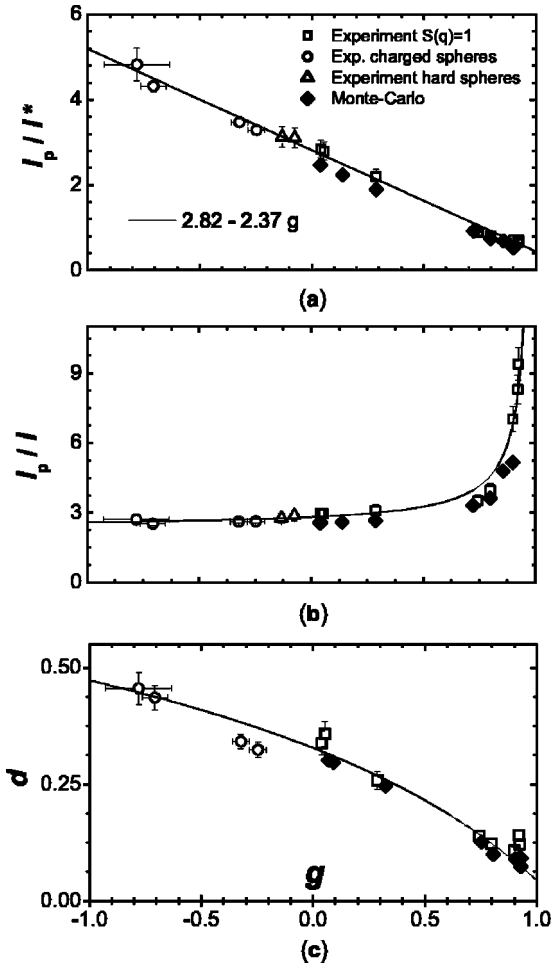

Fig. 4. (a), (b) Depolarization length l_p from DWS measurements and Monte Carlo simulations: (squares) measurements for different particle sizes (random particle configuration $S(q) \equiv 1$), (circles) strongly interacting charged particles,[18] (triangles) hard-sphere data from Ref. 27, (Diamonds) Monte Carlo simulations. (c) Depolarization ratio directly obtained from the measured intensities. The curves are calculated from the linear fit to l_p/l^* shown in (a).[4,22]

surprising to see that in Fig. 4 l_p scales as in the Rayleigh limit, i.e., $l_p \simeq 3l$, even for a transport mean free path $l^* \simeq l/2$. When l_p/l^* is plotted as a function of g, we find an almost linear behavior over the full accessible range. At this point our understanding of l_p is limited to the particular cases ($g = 0$, $g = 1$, and $g = -1$); a more detailed, microscopic approach would be required to explain the complete dependence of l_p on g or the dependence on other single-particle optical properties.

5. DEPOLARIZATION RATIO OF BACKSCATTERED INTENSITIES

An alternative way to study polarization of multiple backscattered waves is through the (full-intensity) depolarization ratio:

$$d = \frac{I_\parallel - I_\perp}{I_\parallel + I_\perp}. \tag{14}$$

This can be written as

$$d = \frac{\int_0^\infty [P_\parallel(s) - P_\perp(s)]\mathrm{d}s}{\int_0^\infty [P_\parallel(s) + P_\perp(s)]\mathrm{d}s} \cong \int_0^\infty \frac{3}{2}\exp(-s/l_p)P(s)\mathrm{d}s, \tag{15}$$

from where we identify an s-dependent depolarization ratio $d(s)$:

$$d(s) \cong \tfrac{3}{2}\exp(-s/l_p). \tag{16}$$

Since $P_\parallel(s) + P_\perp(s) = P(s)$ and $\int_0^\infty P(s)\mathrm{d}s = 1$, we therefore have

$$\begin{aligned} d &= \int_0^\infty P(s)d(s)\mathrm{d}s \\ &\cong \tfrac{3}{4}\{\exp[-\gamma_p(3l^*/l_p)^{1/2}] + \exp[-(\gamma_p + 2\gamma_e) \\ &\quad \times(3l^*/l_p)^{1/2}]\}. \end{aligned} \tag{17}$$

Thus from the measured intensities $I_\parallel$ and $I_\perp$ it is possible to estimate l_p. In Fig. 4(c) we show the experimental values of d. Again the agreement is excellent over the full accessible range. The data come very close to the predicted values in the three particular cases: $d = 0.33$ for Rayleigh scattering ($g = 0$), $d = 0.14$ for forward-peaked scattering ($g = 1$), and $d = 0.49$ for backward-peaked scattering ($g = -1$).

6. CONCLUSION

In this paper we have shown how to describe the effect of the scattering anisotropy on the depolarization of linearly polarized light and how to use diffusing wave spectroscopy to determine the characteristic depolarization properties. By means of numerical simulations, we checked the limit of validity of the diffusion approximation when the scattering anisotropy g is increased, and we have shown how to correct the predictions by means of an anisotropy-dependent cutoff for the path-length distribution $P(s)$. We discuss for the first time the dependence of the characteristic depolarization length over the full range of possible values of g, including the unusual case of negative g values. In our description the extrapolation length γ is a well-defined constant, as required by diffusion theory. Our work thus clarifies the meaning of γ, a subject of intense discussion in the past.[28–30] Since our description uses only a single adjustable parameter, it is now possible to fully characterize backscattered light with polarization-resolved measurements. We think that this approach can strongly benefit applications in the field of soft-materials and biomaterials analysis, as well as diffuse light imaging techniques.[1,13,31]

ACKNOWLEDGMENTS

We thank D. J. Pine, M. Cloitre, A. Maggs, F. Jaillon, and V. Rossetto for discussions. Financial support from the Swiss National Science foundation is gratefully acknowledged.

Correspondence should be addressed to Frank Scheffold (e-mail, Frank.Scheffold@unifr.ch).

REFERENCES AND NOTES

1. D. A. Weitz and D. J. Pine, in *Dynamic Light Scattering*, W. Brown, ed. (Oxford U. Press, New York, 1993), Chap. 16, pp. 652–720.
2. G. Maret and P. E. Wolf, "Multiple light-scattering from disordered media—the effect of Brownian motion of scatterers," Z. Phys. B **65**, 409–431 (1987).
3. D. J. Pine, D. A. Weitz, P. M. Chaikin, and E. Herbolzheimer, "Diffusing-wave spectroscopy," Phys. Rev. Lett. **60**, 1134–1137 (1988).
4. R. Lenke and G. Maret, in *Multiple Scattering of Light: Coherent Backscattering and Transmission*, W. Brown, ed. (Gordon & Breach, Reading, UK, 2000), pp. 1–72.
5. E. Akkermans, P. E. Wolf, R. Maynard, and G. Maret, "Theoretical study of the coherent backscattering of light by disordered media," J. Phys. (Paris) **49**, 77–98 (1988).
6. E. E. Gorodnichev, A. I. Kuzovlev, and D. B. Rogozkin, "Diffusion of circularly polarized light in a disordered medium with large-scale inhomogeneities," JETP Lett. **68**, 22–28 (1998).
7. F. C. MacKintosh, J. X. Zhu, D. J. Pine, and D. A. Weitz, "Polarization memory of multiply scattered light," Phys. Rev. B **40**, 9342–9345 (1989).
8. F. C. MacKintosh and S. John, "Diffusing-wave spectroscopy and multiple scattering of light in correlated random media," Phys. Rev. B **40**, 2383–2406 (1989).
9. D. Bicout, C. Brosseau, A. S. Martinez, and J. M. Schmitt, "Depolarization of multiply scattered waves by spherical diffusers: influence of the size parameter," Phys. Rev. E **49**, 1767–1770 (1994).
10. V. L. Kuzmin and V. P. Romanov, "Multiply scattered light correlations in an expanded temporal range," Phys. Rev. E **56**, 6008 (1997).
11. D. Lacoste, V. Rossetto, F. Jaillon, and H. Saint-Jalmes, "Geometric depolarization in patterns formed by backscattered light" Opt. Lett. (to be published).
12. D. A. Zimnyakov, Y. P. Sinichkin, P. V. Zakharov, and D. N. Agafonov, "Residual polarization of non-coherently backscattered linearly polarized light: the influence of the anisotropy parameter of the scattering medium," Waves Random Media **11**, 395–412 (2001).
13. A. D. Kim and J. B. Keller, "Light propagation in biological tissue," J. Opt. Soc. Am. A **20**, 92–98 (2003).
14. M. Moscoso, J. B. Keller, and G. Papanicolaou, "Depolarization and blurring of optical images by biological tissue," J. Opt. Soc. Am. A **18**, 948–960 (2001).
15. P. Sebbah, *Waves and Imaging through Complex Media* (Kluwer Academic, Dordrecht, The Netherlands, 2001).
16. H. C. van de Hulst, *Light Scattering by Small Particles* (Dover, New York, 1981).
17. C. F. Bohren and D. R. Huffman, *Absorption and Scattering of Light by Small Particles* (Wiley, New York, 1983).
18. L. F. Rojas-Ochoa, J. M. Mendez-Alcaraz, J. J. Saenz, P. Schurtenberger, and F. Scheffold, "Photonic properties of strongly correlated colloidal liquids" Phys. Rev. Lett. (to be published). We note that in the present work we did not study concentrations above $\Phi = 7.4\%$ on account of a slow and streched long-time decay observed in this supercooled or glassy state. Note that these effects show up much more pronounced in backscattering DWS as compared with the transmission geometry studied previously.
19. A. Ishimaru, *Wave Propagation and Scattering in Random Media* (Academic, New York, 1978).
20. A. Lagendijk, R. Vreeker, and P. DeVries, "Influence of internal reflection on diffusive transport in strongly scattering media," Phys. Lett. A **136**, 81–88 (1989).
21. J. X. Zhu, D. J. Pine, and D. Weitz, "Internal reflection of diffusive light in random media," Phys. Rev. A **44**, 3948–3959 (1991).
22. R. Lenke and G. Maret, "Magnetic field effects on coherent backscattering of light," Eur. Phys. J. B **17**, 171–185 (2000).
23. R. Lenke, R. Tweer, and G. Maret, "Coherent backscattering of turbid samples containing large Mie spheres," Pure Appl. Opt. **4**, 293–298 (2002).
24. A. C. Maggs and V. Rossetto, "Writhing photons and Berry phases in polarized multiple scattering," Phys. Rev. Lett. **87**, 253901 (2001).
25. A. H. Hielscher, A. A. Eick, J. R. Mourant, D. Shen, J. P. Freyer, and I. J. Bigio, "Diffuse backscattering Mueller matrices of highly scattering media," Opt. Express **1**, 441–453 (1997); www.opticsexpress.org.
26. A. G. Yodh, P. D. Kaplan, and D. J. Pine, "Pulsed diffusing-wave spectroscopy—high resolution through nonlinear optical gating," Phys. Rev. B **42**, 4744–4747 (1990).
27. L. F. Rojas-Ochoa, S. Romer, F. Scheffold, and P. Schurtenberger, "Diffusing wave spectroscopy and small-angle neutron scattering from concentrated colloidal suspensions," Phys. Rev. E **65**, 051403 (2002).
28. M. Rosenbluh, M. Hoshen, I. Freund, and M. Kaveh, "Time evolution of universal optical fluctuations," Phys. Rev. Lett. **58**, 2754–2757 (1987).
29. I. Freund and M. Kaveh, "Comment on 'Polarization memory of multiply scattered light'," Phys. Rev. B **45**, 8162–8163 (1992).
30. F. C. MacKintosh, J. X. Zhu, D. J. Pine, and D. A. Weitz, "Reply to 'Comment on "Polarization memory of multiply scattered light"'," Phys. Rev. B **45**, 8165 (1992).
31. F. Scheffold, "Particle sizing with diffusing wave spectroscopy," J. Dispersion Sci. Technol. **23**, 591–599 (2002).